

# A Synthetic Strand of Cardiac Muscle

## *Its Passive Electrical Properties*

MELVYN LIEBERMAN, TOHRU SAWANOBORI,  
J. MAILEN KOOTSEY, and EDWARD A. JOHNSON

From the Department of Physiology, Duke University Medical Center, Durham, North Carolina 27710. Dr. Sawanobori's present address is the Department of Clinical Physiology, Tokyo Medical and Dental University, Tokyo, Japan.

**ABSTRACT** The passive electrical properties of synthetic strands of cardiac muscle, grown in tissue culture, were studied using two intracellular microelectrodes: one to inject a rectangular pulse of current and the other to record the resultant displacement of membrane potential at various distances from the current source. In all preparations, the potential displacement, instead of approaching a steady value as would be expected for a cell with constant electrical properties, increased slowly with time throughout the current step. In such circumstances, the specific electrical constants for the membrane and cytoplasm must not be obtained by applying the usual methods, which are based on the analytical solution of the partial differential equation describing a one-dimensional cell with constant electrical properties. A satisfactory fit of the potential waveforms was, however, obtained with numerical solutions of a modified form of this equation in which the membrane resistance increased linearly with time. Best fits of the waveforms from 12 preparations gave the following values for the membrane resistance times unit length, membrane capacitance per unit length, and for the myoplasmic resistance:  $1.22 \pm 0.13 \times 10^6 \Omega\text{cm}$ ,  $0.224 \pm 0.023 \mu\text{F}\cdot\text{cm}^{-1}$ , and  $1.37 \pm 0.13 \times 10^7 \Omega\text{cm}^{-1}$ , respectively. The value of membrane capacitance per unit length was close to that obtained from the time constant of the foot of the action potential and was in keeping with the generally satisfactory fit of the recorded waveforms with solutions of the cable equation in which the membrane impedance is that of a single capacitor and resistor in parallel. The area of membrane per unit length and the cross-sectional area of myoplasm at any given length of the preparation were determined from light and composite electron micrographs, and these were used to calculate the following values for the specific electrical membrane resistance, membrane capacitance, and the resistivity of the cytoplasm:  $20.5 \pm 3.0 \times 10^3 \Omega\text{cm}^2$ ,  $1.54 \pm 0.24 \mu\text{F}\cdot\text{cm}^{-2}$ , and  $180 \pm 34 \Omega\text{cm}$ , respectively.

### INTRODUCTION

In cardiac muscle, as in other excitable cells, the passive electrical properties of the cell membrane and cytoplasm must be determined from observations of

the electrical behavior of the cell or tissue as a whole: e.g., measurements of displacements in transmembrane potential and the currents that are used to cause them. The task is greatly simplified if the shape of intracellular space conforms to some simple geometry, in which case useful equations can be derived which relate the current injected and the magnitude of the potential displacements at a point to the specific impedance of the membrane and cytoplasm.

The functional anatomy of cardiac muscle is far more complex than skeletal muscle or nerve, the fibers of which function individually and behave, in many cases of interest, as one-dimensional leaky capacitive cables. The masses of closely packed, short, roughly cylindrical cells that make up the walls of the heart, form complicated three-dimensional networks of electrically contiguous cells through resistive intercellular connections in regions of close membrane apposition. Even in structures as simple as a single, tiny, free-running bundle of fibers, such networks do not fit any particular pattern (1).

In the past, although such complexity may have been recognized, it appears to have been considered of minor importance, presumably for the sake of theoretical simplicity. The custom has been to choose a geometrical model that resembles the gross rather than the fine anatomy of the preparation, or else the fine structure has been presumed to conform to one of several simple patterns to which a useful theoretical treatment could, or had already been applied.

For example, stacks of closely packed, interdigitating Purkinje cells from unguulate hearts have been treated, electrically, as a single cylindrical cell and the electrical constants obtained using the classical formulae of one-dimensional cable theory as originally applied to nerve (e.g. 2-4). It is not obvious that these simplifying assumptions are justified, and the arguments and evidence in support of them have never been explicitly presented. Indeed, it has been inferred (arguments to the contrary, cf. Discussion, aside) that in Purkinje bundles from hearts of smaller animals, where the complexity of fiber interconnections was found to be much simpler (i.e. splitting into daughter bundles did not occur), no relationship can uniquely relate the input impedance of a fiber to the impedance of the membrane and cytoplasm (1).

Other preparations of cardiac muscle, such as the wall of the atrium and ventricle, have been considered as an extensive thin-plane cell (5-7), or as a hexagonal (8, 9) or square-lattice array (9-11) of interconnecting one-dimensional cells (for general review, see 12, 13). These models again oversimplify the true geometry since the actual input impedance of the tissue depends critically on the true form of intracellular space in the immediate vicinity of the site of current injection. In practice, the form of this space is neither predictable nor readily determined and only as a crude approximation does it approach the shapes or patterns of such simple geometries.

The need for a simple preparation of cardiac muscle, free of complexities

and uncertainties of this kind, stems not only from the wish to obtain precise values for the specific electrical constants of cardiac muscle, but also from the wish to apply the analytic technique of voltage clamp to determine the non-linear electrical properties of the membrane. With an experimental preparation having a geometry which could be faithfully described, mathematically, we could simulate the voltage-clamp experiments including the effects of spatial variations in membrane potential and their effects on the experimental results (14). Our idea is that we might thereby separate those aspects of the results which arise from inhomogeneities of membrane potential control from those which originate from membrane properties. Our inability to find a naturally occurring preparation satisfying our criteria of simplicity (15, 16) drove us to explore the feasibility of growing in tissue culture an artificial preparation of cardiac muscle which would conform to a desired geometry, e.g. a single column of cells. In developing culture techniques that would accomplish this aim, a prototype preparation was developed: a tiny bundle of fibers which could be grown to any desired length (17). Unlike its naturally occurring counterpart, the synthetic strand proved to be readily amenable to study with intracellular microelectrodes, perhaps because of the relatively rigid mechanical support along its entire length and only unorganized traces of collagen (18). Preliminary electrical findings showed that the preparation seemed to behave as a single one-dimensional cable (19, 20),<sup>1</sup> and for this reason we were encouraged to complete a full detailed analysis of its passive electrical properties. The results are presented here together with the morphometry necessary to translate the cable parameters into values for the specific electrical constants.

#### METHODS

##### *Preparation*

Synthetic strands of cardiac muscle were made by directing the growth of isolated embryonic chick heart cells in linear arrays (17). In brief, the hearts from 11- to 13-day old chick embryos were removed, minced, and disaggregated at 37°C in a solution of 0.1 % trypsin-Saline G for 10 min. The cells were resuspended in conditioned medium and seeded at known densities ( $2.5 \times 10^4$ – $1.0 \times 10^5$  cells/cm<sup>2</sup>) on agar-coated culture dishes in which channels were cut (approximately 25  $\mu$ m wide) in the agar film. The cultures were incubated from 3 to 11 days at 37°C in a humidified chamber containing 5 % CO<sub>2</sub> and 95 % air. The culture medium was Medium 199 in modified Earle's balanced salt solution containing 10 % fetal calf serum, 2 % chick embryo extract, and a 1 % mixture of penicillin G and streptomycin sulfate. The concentrations for Na<sup>+</sup>,

<sup>1</sup> During the preparation of this manuscript, our attention was drawn to the Ph.D. thesis of Frederick Sachs (Department of Physiology, State University of New York, Upstate Medical Center, Syracuse, N. Y.) in which he undertook a cable analysis of tissue-cultured heart cells grown in a linear array.

$K^+$ ,  $Ca^{++}$  ions were determined by flame photometry (model 21, Coleman Instruments Div., Perkin Elmer Corp., Oak Brook, Ill.) for all the media, and the mean values were as follows (meq/liter):  $Na^+$ , 152;  $K^+$ , 5.4;  $Ca^{++}$ , 3.2. Osmolarity of the media was measured (Osmette, Precision Systems, Sudbury, Mass.) and the mean value of all media was 311 mosmol/kg  $H_2O$ .

The strands typically selected for these studies by light microscopic examination were spontaneously active, uniform in width along a length greater than 1.0 cm, and bounded by naturally occurring ends. A photomicrograph of a segment of one such preparation is shown in Fig. 1 A. Previous studies by Purdy et al. (18) have shown that when such a strand is cut in cross section and examined with electron microscope, it approximates a right circular cylinder consisting of an inner core of muscle cells surrounded by an annulus of epimysium. A schematic reconstruction of one of the strands used to obtain several of the measured parameters described in the following section is illustrated in Fig. 1 B.

#### *Morphometry*

Dimensional analyses of the synthetic strands were obtained from light and electron microscopic photographs of living and fixed preparations. The average overall radius,  $a$ , of each living strand was determined from composite photomicrographs (for details, see [19]), the overall diameter of each preparation being measured at 50- $\mu m$  intervals along a length bounded by the extreme positions of the stimulating and most distant recording electrodes. From this value of  $a$ , the radius of the muscle core for each preparation was estimated by subtracting an average value for the thickness of epimysium,  $\epsilon$ . The value of  $\epsilon$  was determined from measurements of the thickness of epimysium made at intervals of 20° in light and composite electron micrographs of cross sections of several preparations (for details, see [18]). In these same preparations, the area of the muscle core,  $\sigma$ , that was calculated from the measured value of  $a$  and estimated value of  $\epsilon$  (see Eq. 2), was in close agreement with the actual cross-sectional area of muscle core obtained by planimetry.

The total length of sarcolemmal profile in the muscle core (uncorrected for membrane folding),  $L_o$ , in the entire cross section of each of two strands was determined by tracing the cell boundaries from electron micrograph montages with a curvometry map-reader. A value for the area of myoplasm in the muscle core (also uncorrected for folding),  $S_o$ , was measured by cutting out and weighing the appropriate regions of the prints. The myoplasmic area per unit cross-sectional area of muscle core,  $\Psi$ , that was calculated from these measured parameters (see Results) closely agreed with values obtained by gravimetric analysis of photomicrographs of the same preparations. The membrane folding factor,  $\phi$ , was calculated by measuring cell contours in enlarged sections of electron micrographic plates that were projected onto a wall screen. The true sarcolemmal length and the length ignoring folding (i.e. the length corresponding to  $L_o$ , above) were measured with a map-reader and a length of thread, respectively. The ratios of these two values, when averaged, gave the average folding factor,  $\bar{\phi}$ .

#### *Electrophysiological Recording*

The electrophysiological methods used in this study have been described in detail elsewhere (19). Fig. 2 is a diagrammatic representation of the preparation and recording

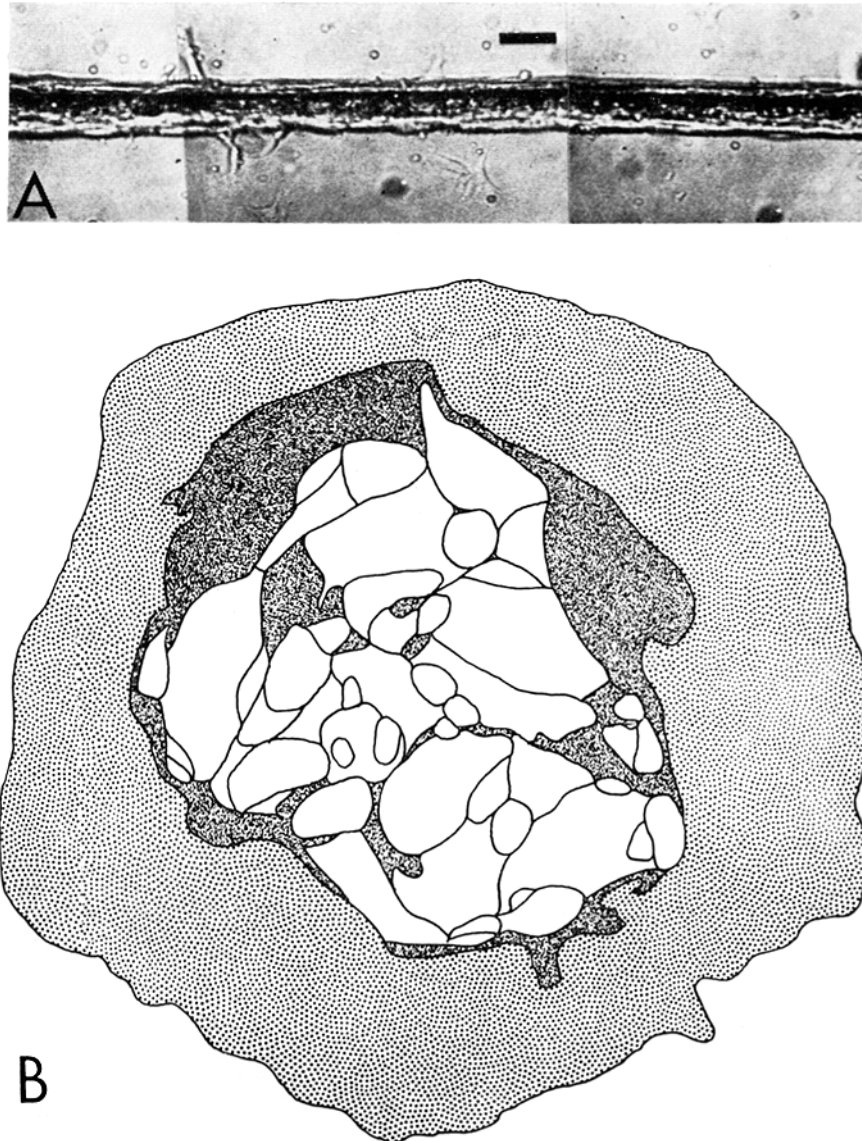


FIGURE 1. A, phase contrast photomicrograph of a segment of a spontaneously active synthetic strand. Scale,  $50\ \mu\text{m} \times 140$ . B, schematic reconstruction of a transverse section of a strand composed from low magnification electron micrographs. Central area outlines the inner core of muscle cells (clear) and extracellular space (shaded), both of which are enveloped by an epimysial annulus (stippled).

apparatus. The strand was stimulated extracellularly once every 630 ms through a bevel-edged glass microelectrode (tip diameter approximately  $50\ \mu\text{m}$ ) filled with 1.5% agar in Saline G. Glass microelectrodes ( $40\text{--}60\ \text{M}\Omega$ ) were used to record transmembrane potential and to inject current into a cell: bipolar reed relays switched the

electrode to either a constant current generator (21) or to a guarded input probe amplifier (22). Two silver wires formed the return and reference electrode for the extracellular stimulation and intracellular microelectrodes, respectively. Rectangular current pulses (50–150-ms duration) were injected via one intracellular microelectrode after every fourth or sixth action potential, approximately 350 ms before the onset of the next action potential (Fig. 3 A). A second intracellular microelectrode recorded the resultant displacement of membrane potential at various distances along the strand away from the current electrode. Conduction velocity was measured as the ratio of the time between the moments at which the rate of depolarization reached a

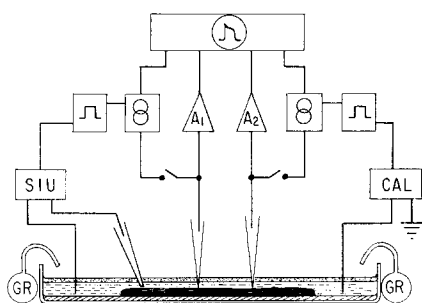


FIGURE 2

FIGURE 2. Diagram of the experimental apparatus. The intracellular microelectrodes are connected to either guarded input probe amplifiers ( $A_1$ ,  $A_2$ ) or constant current generators ( $\theta$ ). SIU, stimulus isolation unit; CAL, voltage calibrator; GR, gassing ring for air/ $\text{CO}_2$  mixture. Culture medium in dish (dashed lines) is overlaid with light mineral oil (stippled).

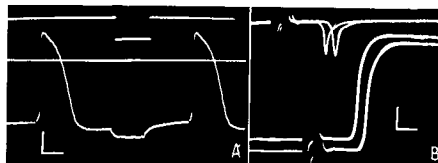


FIGURE 3

FIGURE 3. A, timing of test pulses; B, measurement of conduction velocity. A, upper trace: current. Middle trace: zero potential. Lower trace: membrane potentials, calibration = 20 mV or 10 nA, 100 ms. B, upper traces: first derivative of membrane potentials. Lower traces: recording from two microelectrodes spaced 1.0 mm apart; calibration = 20 mV or 20  $\text{V} \cdot \text{s}^{-1}$ , 10 ms.

maximum in action potentials recorded at two points divided by the distance between them (Fig. 3 B).

#### Numerical Computation

The partial differential equation

$$\frac{1}{r_i} \frac{\partial^2 V}{\partial x^2} - c_m \frac{\partial V}{\partial t} - \frac{V}{r_m(t)} = I(t), \quad (1)$$

was solved numerically by the Crank-Nicolson implicit method (23). A total preparation length of 5 mm (approximately 5 length constants) was simulated in 100 segments by choosing the length increment  $\Delta x$  to be 0.05 mm. The time increment at  $\Delta t$  was chosen for each integration to make the mesh ratio  $\Delta t / (r_i c_m [\Delta x]^2)$  equal to 1; a typical value of  $\Delta t$  was 75  $\mu\text{s}$ .

Numerical solutions of Eq. 1 were fitted to the experimental data by constructing an error function relating the solutions and data and finding values of the parameters  $r_i$ ,  $r_m$ ,  $c_m$ , and  $\alpha$  which minimized this error function. The families of experimental curves were enlarged photographically and voltages were read off at 25 values of time for each electrode distance (see Results). The error function was then equal to the sum of the absolute values of the differences between the measured and calculated voltages at each time and position. An algorithm similar to that of Powell (24) was used to minimize the error function and was chosen because it did not require a knowledge of the derivatives of the error function.

## DEFINITIONS

*Symbols for Morphometry*

- $a$  overall radius of the strand (cm).  
 $\epsilon$  thickness of epimysium (cm).  
 $L_o$  curvimetered length of sarcolemmae (cm).  
 $S_o$  measured area of muscle core (cm<sup>2</sup>).  
 $\phi$  membrane folding factor.  
 $\sigma$  cross-sectional area of muscle core (cm<sup>2</sup>).  
 $L$  sarcolemmal length in muscle core (cm).  
 $\beta$  sarcolemmal length per unit cross-sectional area of muscle core (cm<sup>-1</sup>).  
 $\Psi$  myoplasmic area per unit cross-sectional area of muscle core.  
 $A$  cross-sectional area of muscle core per unit length of preparation (cm<sup>2</sup>·cm<sup>-1</sup>).  
 $S$  myoplasmic area in muscle core (cm<sup>2</sup>).

*Relevant Morphometric Equations*

The following equations were used to derive the morphometric parameters that were used in the derivation of the membrane parameters. Super-bar (—) over any morphometric variable denotes average values obtained from preparations.

$$\sigma = \pi(a - \bar{\epsilon})^2. \quad (2)$$

$$L = \phi L_o. \quad (3)$$

$$\beta = L/\sigma. \quad (4)$$

$$\Psi = S_o/\sigma. \quad (5)$$

$$A = \bar{\beta}\bar{\sigma}\bar{\phi}. \quad (6)$$

$$S = \bar{\Psi}\sigma. \quad (7)$$

*Symbols for Cable Parameters*

- $V$  displacement of membrane potential (V).  
 $I(t)$  applied current;  $I = 0$  for  $t \leq 0$ ,  $I = I_o$  for  $t > 0$ ; ( $A$ ).  
 $x$  distance along the strand from point of current injection (cm).  
 $t$  time (s).  
 $r_i$  resistance of myoplasm per unit length ( $\Omega\text{cm}^{-1}$ ).

$r_m$	membrane resistance times unit length at any time, $t$ ; $\bar{r}_m$ is value at start of current pulse, $t = 0$ ; ( $\Omega\text{cm}$ ).
$c_m, c_{AP}$	membrane capacitance per unit length ( $\text{F} \cdot \text{cm}^{-1}$ ).
$\alpha$	time rate of change of membrane resistance ( $\text{s}^{-1}$ ).
$T_{AP}$	time constant of the foot of the action potential (s).
$\theta$	conduction velocity ( $\text{cm} \cdot \text{s}^{-1}$ ).
$R_o$	slope of input current-voltage relationship ( $\Omega$ ).
$R_i$	volume resistivity of the myoplasm ( $\Omega\text{cm}$ ).
$R_m$	specific resistance of membrane at any time, $t$ ; $\bar{R}_m$ is value at start of current pulse, $t = 0$ ; ( $\Omega\text{cm}^2$ ).
$C_m$	specific capacitance of membrane ( $\text{F} \cdot \text{cm}^{-2}$ ).

## RESULTS

### *Electrical*

Fig. 4 shows typical examples of the change in membrane potential produced by a rectangular pulse of hyperpolarizing current recorded at increasing distances from the site of injection of current. In all instances, the displacements in membrane potential produced by the current were not from a fixed resting potential because all preparations showed diastolic depolarization characteristic of pacemaker cells (see Fig. 3 A). Assuming that the basic mechanisms underlying this slow depolarization are unaffected by the current and/or displacement of potential from its natural time-course, the potential change of interest is the displacement in membrane potential obtained by subtracting the potential during the current pulse from that during its absence.

This procedure and its results are illustrated in Fig. 5: oscillographs of the time-course of membrane potential during and in the absence of the current pulse, for all experiments, were projected and the borders of the traces were outlined. The displacement in membrane potential at any time during the pulse was determined as the difference in potential measured from points midway between the outlines of the potential traces in the presence and absence of current. The time of onset of current was taken as the border outlining the break in the potential trace as indicated in the figure. In this way, the time-course of change in potential displacement during the current pulse was reconstructed for each of the several recording sites distant from the current electrode.

In these, as in all other such records, the potential displacement, instead of approaching a steady value as would be expected for a cell with constant electrical properties, increased slowly with time throughout the current step. A creep in potential such as this has been recorded by others, both in cardiac muscle (2, 25, 26), especially in those preparations that were pacemaking (such as ours), as well as in skeletal muscle (27).



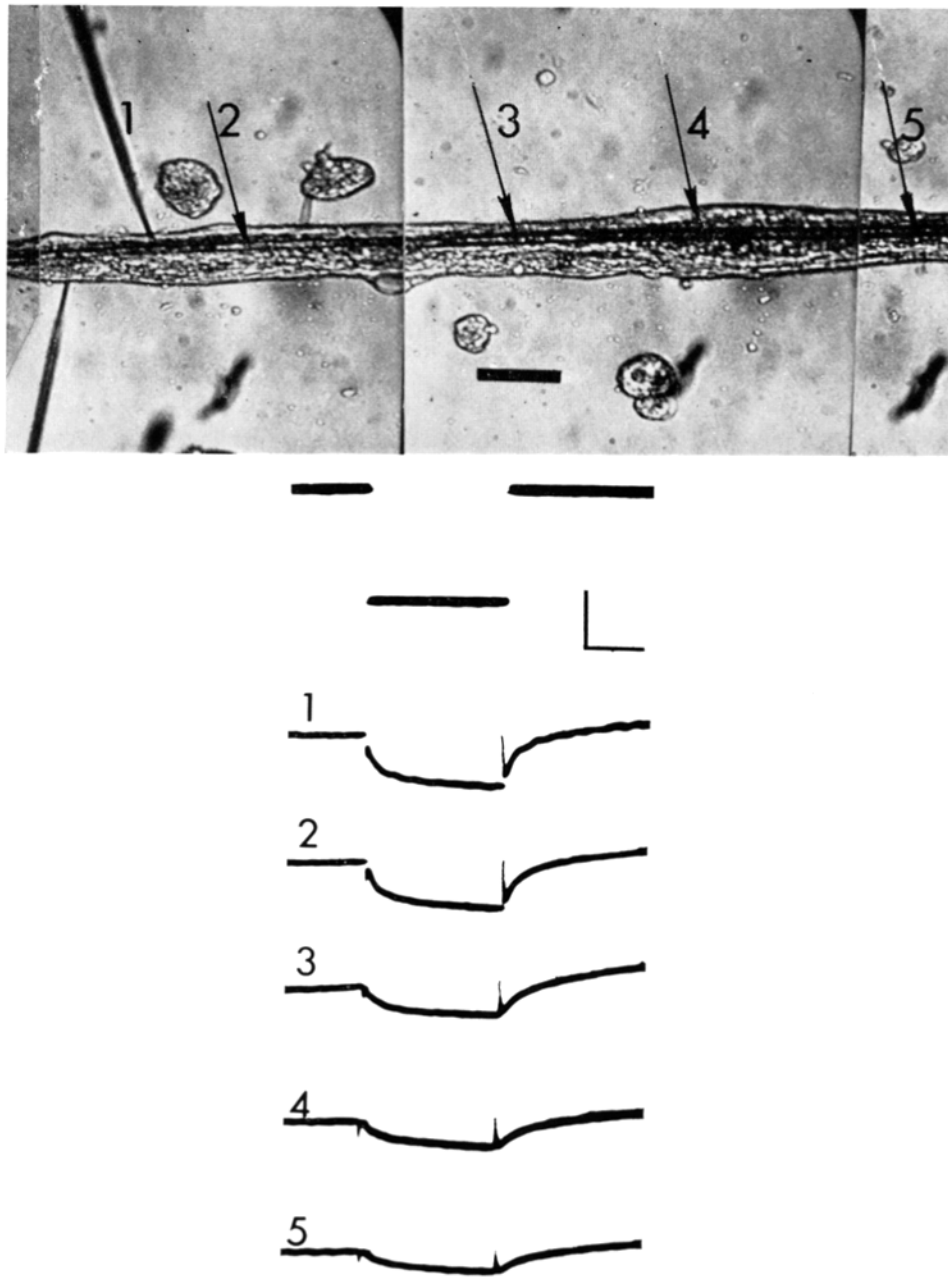


FIGURE 4. Membrane potentials recorded at increasing distances from the site of injection of a rectangular pulse of hyperpolarizing current. Numbered potentials correspond, respectively, to the positions of the recording microelectrode indicated in the photomicrograph. Calibration = 10 nA or 20 mV, 50 ms.

In most preparations, the magnitude of the displacement at a given time (e.g. the end of the current pulse) varied linearly with that of the applied current, up to the maximum value recorded of approximately 30 mV (Fig. 6), although in a few instances the relationship curved slightly at the higher potentials, the slope resistance increasing with potential. The linearity

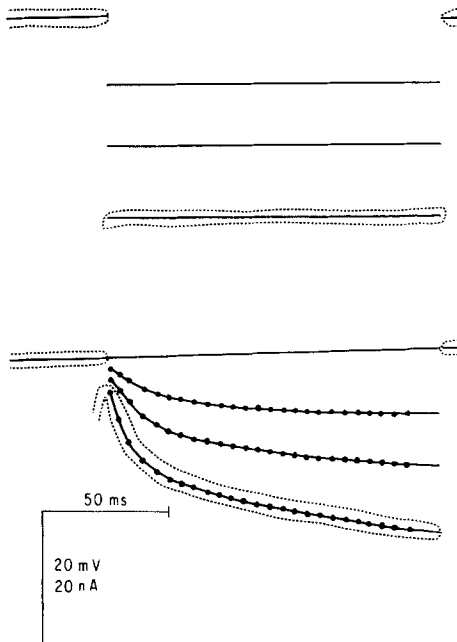


FIGURE 5

FIGURE 5. Example of procedure for obtaining the displacements in membrane potential. The solid points in the lower panel are midway between the upper and lower outlines of the corresponding photographic traces (the solid lines were hand-drawn through these points). See text for further explanation.

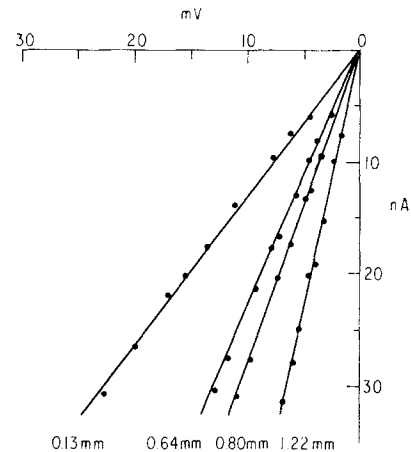


FIGURE 6

FIGURE 6. Current-voltage relationship at various distances from the site of injection of hyperpolarizing currents. Ordinate: current intensity (nA). Abscissa: displacement of membrane potential (mV).

of the current-voltage relationship suggested that the creep in potential could be accounted for by a time-dependent (but voltage- and current-independent) increase in membrane resistance. A similar time dependent increase in membrane resistance has been said to underlie diastolic depolarization in pace-making fibers (28, 29).

Nonetheless, whatever its true cause, the creep is clearly a serious obstacle in determining the passive electrical properties of the preparation (2). The usual methods that are applicable to the geometry of our preparations are based on the analytic solution of the partial differential equation describing a

one-dimensional cell with constant electrical properties. Clearly, potential waveforms with creep of the magnitude found in our experiments (and for matter found by others) cannot be fitted with such solutions. Indeed, until shown otherwise, the use, in such circumstances, of the classical formulae derived from these solutions to obtain values for the cable parameters is invalidated.

The only recourse is to attempt to obtain a satisfactory fit of the waveforms of potential displacement by assuming some additional factor that will account for the slow creep in potential. As pointed out above, a time-dependent increase in  $r_m$  could be such an assumption. A plot of  $R_o^2$  as a function of time during the latter part of the current pulse suggests, intuitively at least, that a linear increase in  $r_m$  as a function of time might prove satisfactory (see Fig. 7).<sup>2</sup>

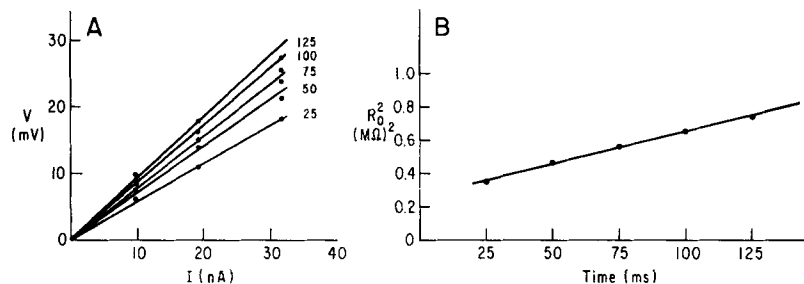


FIGURE 7. A, current-voltage relationship plotted for different times during creep in potential. B, a plot of the square of the slope ( $R_o$ ) of the current-voltage relationships as a function of time during the current step.

Unfortunately, we were unable to find an analytic solution of Eq. 1. The families of waveforms of potential displacement of the kind shown in Fig. 5 were therefore fitted with numerical solutions of Eq. 1, with  $r_m(t) = \bar{r}_m(1 + \alpha t)$ ,  $\alpha$  being a constant for each preparation and  $\bar{r}_m$  the initial value of  $r_m$  at the start of the current pulse ( $t = 0$ ) and where  $r_i$ ,  $c_m$ ,  $V$ , and  $x$  are as defined in Definitions. The values of these parameters were chosen to give an overall best fit to each family of waveforms (see Methods).

The quality of the fit to 12 families of waveforms from 12 preparations ranged from poor to good (see Fig. 8). The best example (Fig. 8 A) demonstrates that the preparation behaved remarkably like a one-dimensional cell, not only at long but also at short times after the point application of a step of

<sup>2</sup> An increase in  $r_i$  as a function of time would have been an equally reasonable assumption in order to account for the creep in potential at one point. The correct choice is decided by the overall fit to the family of waveforms, for an increasing  $r_m$  causes the "length constant" to increase with time whereas an increasing  $r_i$  causes it to decrease. We do not wish to suggest that the success of this simple assumption (cf. Fig. 8) be taken as evidence that  $r_m$  could not, in fact, be voltage as well as time dependent.

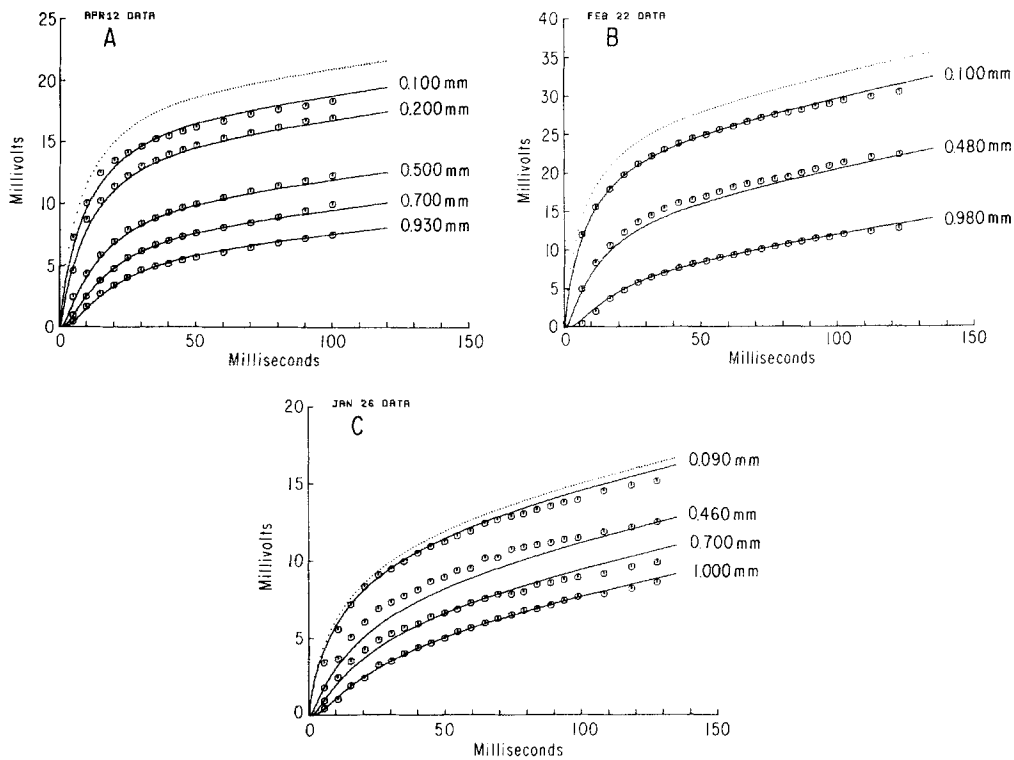


FIGURE 8. Theoretical fit of displacements of membrane potential recorded experimentally at various distances from the site of injection of a step of hyperpolarizing current. Solid lines: theoretical curves fitted to experimental points,  $\square$ . Dotted line: theoretical curve for zero electrode separation. Panels A, B, and C are examples of good, fair, and poor fits, respectively.

hyperpolarizing current. In other preparations, the fit was less satisfactory (see Fig. 8 B, C). The deviation at short times was almost invariably of the kind shown in Fig. 8 C, and is reminiscent of that seen when a component part of the membrane capacitance is in series with a substantial resistance, as, for example, in skeletal muscle (30) and Purkinje strands from ungulate hearts (3). Except for the latter, this property in cardiac muscle most likely originates not from the membrane itself or from a finely distributed second system of membrane (e.g. in the form of transverse tubules or clefts), but from the multi-fibered nature of the preparation (1, 15). Clefts or transverse tubules, when present, are too short or too large to be effectively isolated from the rest of the membrane. If the frequency and distribution of resistive connections between cells is insufficient to smooth out the discontinuity introduced by the discreteness of such connections, the fibers can behave locally as a cable terminated, more or less, at one point by a number of cables. The equivalent circuit

of this case is identical to that which would fit waveforms of the kind shown in Fig. 8 C.

The values of  $c_m$ ,  $\bar{r}_m$ ,  $r_i$ , and  $\alpha$  for the best fits are given in Table I.<sup>3</sup> In order to convert these values of  $c_m$ ,  $\bar{r}_m$ , and  $r_i$  to the corresponding values for the specific cable parameters,  $C_m$ ,  $\bar{R}_m$ , and  $R_i$ , two morphological quantities must be determined for each preparation, namely: the area of membrane per unit length,  $A$ , and the cross-sectional area of myoplasm at any given length,  $S$

TABLE I  
CABLE PARAMETERS AND SPECIFIC ELECTRICAL CONSTANTS  
OF A SYNTHETIC STRAND

Preparation	Age	$a$	$A$	$S$	$\alpha$	$r_i$	$\bar{r}_m^*$	$c_m$	$R_i$	$\bar{R}_m^*$	$C_m$	Stimu- lus
	days	$\mu m$	$cm^2 \cdot cm^{-1}$	$10^{-6} cm^2$	$ms^{-1}$	$10^7 \Omega cm^{-1}$	$10^5 \Omega cm$	$\mu F \cdot cm^{-1}$	$\Omega \cdot cm$	$10^8 \Omega cm^2$	$\mu F \cdot cm^{-2}$	$nA$
1-11-24†	5	35	0.191	1.45	0.0051	0.77	0.71	0.383	112	13.5	2.01	20
1-12-14	4	29	0.110	0.84	0.0044	1.80	1.67	0.171	151	18.4	1.55	33
2-1-13	5	33	0.165	1.23	0.0051	1.64	1.47	0.148	202	24.3	0.90	30
2-1-25	4	35	0.183	1.39	0.0054	1.30	2.16	0.125	181	39.5	0.68	30
2-1-26	5	41	0.293	2.23	0.0166	0.84	1.03	0.249	186	30.2	0.85	20
2-2-3	6	33	0.155	1.18	0.0075	1.46	1.64	0.176	172	25.4	1.14	30
2-2-10	6	31	0.135	1.02	0.0067	1.79	1.25	0.219	183	16.9	1.62	32
2-2-22	11	42	0.313	2.38	0.0106	2.22	1.12	0.131	528	35.1	0.42	29
2-2-29	4	29	0.110	0.84	0.0137	0.66	1.10	0.239	56	12.1	2.18	38
2-4-11	4	33	0.155	1.18	0.0066	1.46	0.73	0.246	172	11.3	1.59	30
2-4-12	5	33	0.162	1.23	0.0020	1.11	0.68	0.351	137	11.0	2.17	30
2-5-23	4	26	0.073	0.56	0.0101	1.37	1.09	0.249	77	8.0	3.41	30
Mean			0.170	1.29	0.0078	1.37	1.22	0.224	180	20.5	1.54	
SEM§			0.020	0.15	0.0012	0.13	0.13	0.023	34	3.0	0.24	

\* Bar represents value at time ( $t = 0$ ).

† Position of current electrode less than 100  $\mu m$  from the natural end of the strand.

§  $\pm$  SEM.

### Morphometry

Ideally, in order to determine the above two morphometric parameters, it would be necessary to measure in each preparation the total sarcolemmal length and the area of myoplasm in every cross section of the preparation throughout its length, a clearly impractical task. Consequently, we determined four factors ( $\bar{\epsilon}$ ,  $\bar{\phi}$ ,  $\bar{\beta}$ ,  $\bar{\Psi}$ ) which allowed us to estimate the value of the two quantities,  $A$  and  $S$ , in any given preparation from the overall radius of that preparation.

<sup>3</sup> The preparations were describable either as an infinite or semi-infinite cable depending on whether the current electrode was positioned effectively at the end or middle of the preparation, an input current equal to half or all of the injected current being the boundary condition appropriate to these two cases, respectively.

The thickness of epimysium was measured in several ways (see Methods) in light microscopic cross sections of several preparations as well as in the two electron micrographic montages referred to below. The thickness was found to be approximately constant ( $10 \mu\text{m}$ ), appearing to be independent of the overall radius of the preparation. A constant value of  $10 \mu\text{m}$  for the factor  $\bar{\epsilon}$  was therefore used in Eq. 2 to determine the cross-sectional area of muscle core,  $\sigma$ , for any given preparation.

In an electron micrographic montage of an entire cross section from each of two preparations, the area of myoplasm in the muscle core  $S_o$ , and the total curvimetered length of sarcolemma,  $L_o$ , were measured (see Methods). The factor,  $\Psi$ , the area of myoplasm per unit cross-sectional area of muscle core was calculated for each of the two montages from Eqs. 2 and 5, using the measured values of  $S_o$  and  $a$ , and the value cited above for the factor,  $\bar{\epsilon}$ . The values obtained for  $\Psi$  for each of the two preparations were 0.71 and 0.76 (mean value of  $\bar{\Psi} = 0.74$ ), i.e. the extracellular space was 29% and 24% in each case (mean value equal to 26%) (see Table II). These values compare favorably with those obtained from inulin space measurements of cat papillary muscle (31) and 11- to 14-day embryonic chick ventricles (32, 33) as well as the Cr-EDTA determination of extracellular space in 18- to 20-day embryonic chick ventricle (34). The factor,  $\beta$ , sarcolemmal length per unit cross-sectional area of muscle core was calculated from Eqs. 2-4 using measured values of

TABLE II  
MORPHOMETRIC DATA: DERIVATION OF FACTORS  $\epsilon$ ,  $\psi$ ,  $\beta$ ,  $\phi$

Preparation	2-2-2	2-3-31	Average*
$a$ , overall radius of strand ( $cm$ )	$2.85 \times 10^{-3}$	$3.35 \times 10^{-3}$	
$\epsilon$ , thickness of annulus of epimysium ( $cm$ )	$1.03 \times 10^{-3}$	$0.95 \times 10^{-3}$	$\bar{\epsilon} = 1.0 \times 10^{-3}$
$L_o$ , curvimetered length of sarcolemmae ( $cm$ )	$82.11 \times 10^{-3}$	$144.17 \times 10^{-3}$	
$S_o$ , measured area of muscle core ( $cm^2$ )	$7.40 \times 10^{-6}$	$13.8 \times 10^{-6}$	
$\phi$ , membrane folding factor (transverse)	1.13	1.08	$\bar{\phi} = 1.11$
$\sigma$ , cross-sectional area of muscle core ( $cm^2$ )	$1.04 \times 10^{-5}$	$1.81 \times 10^{-5}$	
$L$ , sarcolemmal length in muscle core ( $cm$ )	$92.78 \times 10^{-3}$	$155.70 \times 10^{-3}$	
$\beta$ , sarcolemmal length per unit cross-sectional area of muscle core ( $cm^{-1}$ )	$8.92 \times 10^3$	$8.60 \times 10^3$	$\bar{\beta} = 8.76 \times 10^3$
$\psi$ , myoplasmic area per unit cross-sectional area of muscle core	0.71	0.76	$\bar{\psi} = 0.74$

\* Value is the average obtained from the two electron micrographic montages.

$L_o$ ,  $a$ , and the value for the folding factor,  $\phi$ , cited below. The values obtained for  $\beta$  in each of the two preparations were  $8.92 \times 10^3 \text{ cm}^{-1}$  and  $8.60 \times 10^3 \text{ cm}^{-1}$  (mean value of  $\bar{\beta} = 8.76 \times 10^3 \text{ cm}^{-1}$ ) (see Table II). These values are comparable to those obtained for the area per volume ratio of frog ventricle (35, 36) and agree very closely with those area per volume values obtained for mass cultures of embryonic chick heart cells (37) as well as embryonic chick right ventricle (34).

The folding factor,  $\phi$ , was required to correct for the error in the curvimetered measurements of sarcolemmal length made from the electron micrographic montages since these micrographs were necessarily of low magnification ( $\times 9,000$ ). As a consequence, many small membrane foldings were below the resolving power of the map measurer that was used to make the measurements of sarcolemmal length. A folding factor,  $\phi$ , for the membrane in the transverse and longitudinal directions was estimated from projected electron micrographic sections (see Methods) and was found to be approximately equal in both directions. The average value of  $\bar{\phi}$  for the longitudinal direction was 1.08 (9 determinations in 4 plates from 1 preparation) whereas the average value for the transverse direction was 1.11 (31 determinations in 15 plates from 2 preparations). No noticeable differences were observed in the membrane folding of superficial fibers and of fibers deep in the preparation. These values are less than the values recently reported for the membrane folding factor of goat Purkinje fibers (38), the difference, however, can no doubt be attributed to differences between the preparations and methods of fixation.

The average overall radius,  $a$ , of each living strand was determined from several measurements of the overall diameter of each preparation along its length (see Methods). These average values are listed in Table I for the 12 preparations. With each of these individual values of  $a$ , the values of the two quantities  $A$  and  $S$  for each preparation were derived using the four factors,  $\bar{\epsilon}$ ,  $\bar{\phi}$ ,  $\bar{\beta}$ ,  $\bar{\Psi}$ , as described in the following section. The individual and average values of these four factors are listed in Table II.

Using Eqs. 2 and 7, the average cross-sectional area of myoplasm in each strand,  $S$ , was derived, from the average measured value of the overall radius of the living strand listed in Table I, together with the factors  $\bar{\epsilon}$  and  $\bar{\Psi}$ . The average area of membrane per unit length of each strand,  $A$ , was derived from the same average overall radius with factors  $\bar{\beta}$ ,  $\sigma$ , and  $\bar{\phi}$  using Eqs. 2 and 6. The resulting values of  $S$  and  $A$  for each of 12 strands, which will be used to derive  $R_i$ ,  $\bar{R}_m$ , and  $C_m$  from  $r_i$ ,  $\bar{r}_m$ , and  $c_m$ , respectively, are listed in Table I.

The need for accurate values of these morphometric parameters in this regard has been discussed for cardiac muscle (13, 38–40) and has recently been nicely demonstrated for skeletal muscle (41). The value of the ratio of surface area of membrane to volume of the strand (obtained from the ratio of  $S$  and  $A$ ) of  $0.88 \mu\text{m}^{-1}$  corresponds to a cell diameter of  $4.5 \mu\text{m}$  (assuming a cylindri-

cal shape cell), which falls within the range of values reported for embryonic heart cells (3–10  $\mu\text{m}$  [18, 42]) and newly hatched chicks (2–7  $\mu\text{m}$  [43]). In frog ventricular fibers, a similar correspondence is to be found between the cell diameter derived from the area per volume ratio (3.0  $\mu\text{m}$  [36]) and that observed histologically (2–5  $\mu\text{m}$  [44]).

#### *Myoplasmic Resistance*

The volume resistivity of the myoplasm was calculated by multiplying each of the values for  $r_i$  (see Table I) by the corresponding calculated value for the cross-sectional area of myoplasm,  $S$ , for each preparation. The values for  $R_i$  so obtained had a mean of  $180 \pm 35 \Omega\text{cm}$  (see Table I). This value is within the range of values obtained by others for frog skeletal muscle (18–22°C [41]) and chick skeletal muscle in tissue culture (35–37°C [45]).

In contrast, for cardiac muscle values of  $R_i$  ranging from 60 to 500  $\Omega\text{cm}$  have been reported for naturally occurring (2, 3, 39, 46) as well as tissue-cultured preparations (47, 48). This large spread is without doubt largely attributable to the varying degree to which the actual geometry of the preparation approached the various simple geometries (cylinder, sheet, etc.) that were assumed in order to calculate the area of myoplasm in any cross section of the preparation and to derive the theoretical relationship between  $R_i$  and the input resistance (see Discussion).

#### *Membrane Resistance*

The specific membrane resistance at the start of the current pulse,  $\bar{R}_m$ , was calculated by multiplying each of the values of  $\bar{r}_m$  by the corresponding calculated value for the area of membrane per unit length,  $A$ , for each preparation as shown in Table I. The average value of  $20.5 \pm 3 \times 10^3 \Omega\text{cm}^2$  is high compared to that found for skeletal muscle ( $3.9\text{--}8.6 \times 10^3 \Omega\text{cm}^2$  [41]) but comparable to that found for slow (30) and smooth (49) muscle fibers. The value is also high compared to earlier estimates of  $R_m$  for cardiac tissue (ca.  $2.0 \times 10^3 \Omega\text{cm}^2$  [2, 3, 50]) as well as those recently obtained (e.g.  $9.0 \times 10^3 \Omega\text{cm}^2$  [39]). These low values for cardiac muscle are no doubt attributable to the fact that the actual area of membrane per unit length of preparation was much greater than that calculated for a right circular cylinder equal in diameter to that of the preparation. This assumption is obviously at variance with histological fact in the case of unguulate Purkinje strands (15, 38) for which many of the earlier estimates of  $R_m$  were made (see Discussion).

#### *Membrane Capacitance*

The specific membrane capacitance,  $C_m$ , was calculated by dividing each of the individual values of  $C_m$  listed in Table I by the corresponding area of membrane per unit length of strand,  $A$ , and was found to be  $1.54 \pm 0.24 \mu\text{F} \cdot \text{cm}^{-2}$ . The previously reported values for  $C_m$  vary widely both for naturally



occurring cardiac muscle ( $0.81\text{--}13.3 \mu\text{F}\cdot\text{cm}^{-2}$  [2, 3, 39, 46, 50]) and tissue-cultured heart cells ( $1.3\text{--}20 \mu\text{F}\cdot\text{cm}^{-2}$  [48, 51]), no doubt for the same reasons mentioned for the equivalently wide variations in  $R_m$ . Furthermore, the area of membrane per unit length of the preparations used in these reports may have been in two components, one being in series with a resistance; as a consequence,  $c_m$  should vary with the method (e.g. rectangular pulse or foot of action potential), all other conditions being equal, as has indeed been shown (3, 4). In the synthetic strand, it would appear from the satisfactory fit of numerical solutions of Eq. 1 that the membrane capacitance is not divided into two such components. This conclusion is supported by the near unity value for the ratio of  $c_m$  as determined by this method and that obtained from the foot of the action potential (see Table III).<sup>4</sup>

TABLE III  
COMPARISON OF MEMBRANE CAPACITANCE MEASUREMENTS FROM  
SQUARE-PULSE METHOD AND FOOT OF ACTION POTENTIAL

	$r_i$	$T_{AP}$	$\theta$	$c_{AP}^*$	$c_m$
	$10^7 \Omega\text{cm}^{-1}$	ms	$\text{cm}\cdot\text{s}^{-1}$	$\mu\text{F}\cdot\text{cm}^{-1}$	$\mu\text{F}\cdot\text{cm}^{-1}$
1-11-24	0.77	0.68	46	0.090	0.383
2-1-25	1.30	0.40	35	0.157	0.125
2-2-10	1.79	0.45	32	0.121	0.219
2-2-22	2.22	0.45	37	0.073	0.131
2-2-29	0.66	0.42	30	0.401	0.239
2-4-12	1.11	0.30	30	0.334	0.351
2-5-23	1.37	0.72	25	0.162	0.249
Mean	—	—	—	0.191 ‡	0.242 ‡
SEM§	—	—	—	0.048	0.037

\* Capacitance per unit length of membrane calculated according to the method of Tasaki and Hagiwara (52) using the form of the equation  $c_{AP} = 1/r_i T_{AP} \theta^2$ .

‡ Ratio of  $c_m/c_{AP} = 1.27$ .

§  $\pm$  SEM.

#### DISCUSSION

The greatest source of error in previous and, potentially, in all estimates of the values of the electrical constants of cardiac muscle arises from the differences between the true and the assumed form of the geometry of the preparation on which the measurements are made. Although all thin sheets of cardiac muscle can be described, as a first approximation, as a continuum of individual, but electrically contiguous cells that form a single thin plane cell, the electrical

<sup>4</sup> How much of the membrane capacitance could be in series with a resistance and yet escape detection by the above analysis cannot be answered definitely at this time, either experimentally or theoretically (classical sine wave analysis, for example, cannot be used because of the time variation of membrane resistance). Were such evidence to become available, this still leaves open the question discussed above of whether the second component is a property of the membrane itself or represents a second system of membranes, etc.

properties that determine the membrane potential displacement are functions of distance from the site of injection of current. The particular forms of these functions (the area of membrane and the cross-sectional area of cytoplasm as functions of distance) depend on the particular form which the assumed frequency and distribution of resistive interconnections between cells is presumed to take (5-13, 47, 48). The actual geometry in a given preparation is unknown; it clearly does not fall into any of the simple patterns previously considered, and it would not be feasible to determine the actual functions by morphometry.

Some of these problems could be circumvented by using current sources designed to reduce the problem from a two- or three- to a one-dimensional field problem: for example, in the case of a sheet-like preparation, an external line source (6) could be used, and, in the case of a thick bundle, the current could be injected effectively into all fibers with a diffuse external source. Unfortunately, however, studies using the latter approach (26, 39, 46) did not include adequate morphometry; questionable assumptions were made in the estimates of the surface area of membrane per unit length, the cross-sectional area of cytoplasm, and the myoplasmic resistivity.

The use of thin, naturally occurring strands from the Purkinje network of ungulate and dog hearts does not necessarily simplify the problem. The morphology may in fact be more complex, as in dog (15), or simpler in a given cross section, as in goat (15). However, the bundles of Purkinje cells are tightly packed together, higgledy-piggledy in the dog, more orderly in the goat (15), effectively separating the membrane capacitance into two components, one on the surface and one in series with an appreciable resistance in the form of the narrow clefts of extracellular space between fibers (3, 4). In addition to the problems associated with ion accumulation and depletion in these clefts (e.g. 53), the individual bundles have been shown to split into daughter bundles (15).

On the other hand, Purkinje strands from hearts of smaller animals such as the rabbit, cat, and guinea pig, do not appear to have these deficiencies: the strands in such bundles are loosely packed, except where adjacent cells form junctional complexes and where, presumably, the cells are resistively interconnected. However, a histological study of serial sections from a Purkinje strand (approximately 200- $\mu$ m length) from the rabbit heart showed that the frequency and distribution of junctional complexes were not sufficiently great or extensive to obliterate, electrically, the multifibered behavior of the preparation (1). When current is injected with a microelectrode, the current may or may not have to travel a considerable distance before finding its way into the other fibers. Thus, no single relationship could exist which would relate the input resistance of that fiber to the specific membrane resistance and capacitance and the resistivity of the cytoplasm, and in the region near the current electrode, the voltage and current distributions would not be

characteristic of a one-dimensional cable. Clearly, at some distance from the site of current injection, sufficient interconnections between fibers would have occurred to cause the current to be distributed such that in a given cross section, the intracellular potential in all fibers would be the same. In this case, the strand should behave from there on as a one-dimensional cable. Attempts to test this hypothesis in rabbit Purkinje strands failed (unpublished observations) because of the difficulty in making successful multiple impalements.

The unpredictable nature of the geometry of naturally occurring cardiac muscle coupled with experimental difficulties of this kind no doubt motivated the exploration of the use of tissue-cultured preparations. Although single isolated cells of cardiac muscle in tissue culture might at first sight seem to be ideal preparations, their small size (100–200  $\mu\text{m}$  long, 3–10  $\mu\text{m}$  wide, and 1–2  $\mu\text{m}$  thick) is a severe limitation. Assuming a value of 30,000  $\Omega\text{cm}^2$  for the specific membrane resistance and 1  $\mu\text{F}\cdot\text{cm}^{-2}$  for the specific membrane capacitance, the input resistance would be between  $10^9 \Omega$  and  $10^{10} \Omega$ , and the input capacitance between 4–30 pF. In order to record accurately such a high input impedance, not only must a tight seal be made between the membrane and electrode at the site of puncture, but also extraordinary precautions must be made to reduce stray input capacitances and great care taken in compensating for the unavoidable shunt capacitance between the electrode and the grounded bathing solution. The difficulty, if not impossibility, of achieving a tight seal, perhaps accounts for the very low resting potentials that have been recorded from such cells (47, 54–57). Indeed, all our attempts to make measurements from single isolated cells have not been satisfactory in spite of using microelectrodes of small tip diameter (resistance, 40–60  $\text{M}\Omega$ ), and a high power microscopic control of several forms of automatic motion for the final insertion of the microelectrode into the cell. Invariably, the cell became vacuolated and developed surface blebs; at best, stunted action potentials were recorded with corresponding low resting potentials, and at other times, only “resting potentials” were obtained which were never greater than 20–30 mV. This range of values is suspiciously similar to the liquid junction potential between KCl-filled microelectrodes and extruded myoplasm (58).

The need for a high input shunt impedance to study the passive electrical properties of such cells precludes the use of two separate microelectrodes, one for current injection and one for voltage measurement: a double-barreled microelectrode or a single dual-purpose microelectrode must be used instead. These techniques employ various procedures to correct for the effects of the so-called “convergence” resistance of the microelectrode, which, as has been pointed out previously, are, or can be, more or less ineffective (59). For example, in using one single-barreled microelectrode, the electrode frequently forms one arm of a Wheatstone bridge. The usual procedure, in this case, has

been to balance the bridge with the electrode situated extracellularly, and the entire "out-of-balance" signal that was recorded when the electrode was inserted into the cell was taken to be due to the addition of the input impedance of the cell into the bridge circuitry (51, 57, 60). However, a large fraction of the change in impedance on moving into the cell is the result not only of a change in the resistivity of the medium into which the tip of the microelectrode is immersed (a fact which has been recognized and accounted for in some studies [6]), but also of a change in geometry of the volume conductor in the immediate neighborhood of the tip of the electrode (59). Unfortunately, more often than not, the correct procedures for balancing the single-electrode bridge (59) or for separating, in general, the true displacement in membrane potential from the total recorded voltage displacement for single- or double-barreled microelectrodes (59) were not used. As a consequence, erroneously high values are obtained for the input resistance which invalidate the resultant values for the electrical constants (e.g. 51, 57).

Multicellular, sheet-like preparations of tissue-cultured cardiac muscle suffer from the same drawbacks as their naturally occurring counterparts: problems arising from the complex geometry of fiber interconnections. These preparations have been treated theoretically as a one-dimensional cell (flat ribbon or cylinder [47, 48, 51, 62]) although perhaps, in some cases, the assembled clusters of myoblasts might have been better described as a thick, plane cell or semi-infinite solid. In addition, such tissue-cultured preparations generally were "contaminated" with nonmuscle cells, and, to further complicate matters, the single-electrode bridge technique was frequently used in some of these studies in a way that was open to the kind of criticism referred to above.

Morphologically, the synthetic strand closely resembles its naturally occurring counterpart: the Purkinje strand from hearts of small mammals (1). The strand has a core of well-differentiated muscle fibers with regions of close fiber apposition displaying similarly well-differentiated nexuses, fascia, and maculae adherentes (18). Electrically, the synthetic strand behaves remarkably like a simple one-dimensional cell: the time-course of displacement in membrane potential in response to a rectangular pulse of current is that of a one-dimensional cell in which the membrane impedance is described by a single resistor and capacitor in parallel. The frequency and distribution of resistive connections between cells are thus apparently sufficient to conceal the multi-fibered nature of this preparation in this form of analysis, at least for electrode separations greater than 100  $\mu\text{m}$ . Inspection of the quasi-electrical wire diagram of the naturally occurring rabbit Purkinje strand (1) suggests that the same would be true for this preparation. However, we recognize that in different circumstances (e.g. shorter distances, activity, or more detailed AC analysis, cf. [63]) this might not be the case and that the cable properties might be better described three-dimensionally.

## CONCLUSION

In its simplest form, the passive electrical behavior of the synthetic strand, in response to a pulse of injected current and at distances greater than 100  $\mu\text{m}$ , is that of a one-dimensional cable in which the membrane impedance is described by a resistor and a capacitor in parallel, permitting us to extract values for the specific electrical constants of the membrane and cytoplasm. The elemental behavior afforded by such simplified shapes of preparations (e.g. cylinder or sphere) is the simplest that we can obtain at the present time. Although far from the ideal of a single, extraordinarily large cell in which intracellular voltage gradients can be effectively abolished by the insertion of a metallic conductor, the preparation is sufficiently simple to permit its simulation: the behavior that is attributable to its geometry could perhaps be separated from that which must be attributed to its membrane.

The contribution which the complex architecture of the ventricular wall gives to its electrical behavior remains a mystery. Perhaps this can be solved by systematic reconstruction in tissue culture, strands could be made to branch and form regular but increasingly complex geometric patterns, and the changes in electrical behavior evoked by this reconstruction could be studied.

The authors wish to thank both Dr. Tom Dessent for his valuable assistance with the computer programs and calculations and Ms. Joyce Purdy for her meticulous efforts in the morphometric analyses. We are grateful to Dr. Johan Vereecke for stimulating analytical discussions. We thank Ms. Anne E. Roggeveen and Mr. Owen Oakeley for their excellent technical assistance.

This research was supported in part by grants from the National Institutes of Health, HL 12157 and HL 11307 and an Established Investigatorship Award from the American Heart Association (71160) to Dr. Lieberman.

Preliminary reports of portions of this work were given at the meeting of the Federation of American Societies for Experimental Biology (20) and at the Fall Meeting of the American Physiological Society (64).

*Received for publication 25 July 1974.*

## REFERENCES

1. JOHNSON, E. A., and J. R. SOMMER. 1967. A strand of cardiac muscle: Its ultrastructure and the electrophysiological implications of its geometry. *J. Cell Biol.* **33**:103.
2. WEIDMANN, S. 1952. The electrical constants of Purkinje fibres. *J. Physiol. (Lond.)*. **118**:348.
3. FOZZARD, H. 1966. Membrane capacity of the cardiac Purkinje fibre. *J. Physiol. (Lond.)*. **182**:255.
4. CARMELIET, E., and J. WILLEMS. 1971. The frequency dependent character of the membrane capacity in cardiac Purkinje fibres. *J. Physiol. (Lond.)*. **213**:85.
5. WOODBURY, J. W., and W. E. CRILL. 1961. On the problem of impulse conduction in the atrium. *In* Nervous Inhibitions. E. Florey, editor. Pergamon Press Ltd., Oxford, England. 124.
6. NOBLE, D. 1962. The voltage dependence of the cardiac membrane conductance. *Biophys. J.* **2**:381.
7. SHIBA, H., and Y. KANNO. 1971. Further study of the two-dimensional cable theory: An electric model for a flat thin association of cells with a directional intracellular communication. *Biophysik.* **7**:295.

8. GEORGE, E. P. 1961. Resistance values in a syncytium. *Aust. J. Exp. Biol.* **39**:267.
9. BERKINBLIT, M. B., S. A. KOVALEV, V. V. SMOLYANINOV, and L. M. CHAILAKHYAN. 1965. Determination of the main electrical characteristics of the myocardium of the frog ventricle. *Biofizika*. **10**:861.
10. BERKINBLIT, M. B., S. A. KOVALEV, V. V. SMOLYANINOV, and L. M. CHAILAKHYAN. 1965. Input resistance of syncytial structures. *Biofizika*. **10**:309.
11. TANAKA, I., and Y. SASAKI. 1966. On the electrotonic spread in cardiac muscle of the mouse. *J. Gen. Physiol.* **49**:1089.
12. CORABOEUF, E. 1969. Resistance measurements by means of microelectrodes in cardiac tissues. In *Glass Microelectrodes*. M. Lavallee, M. Schanne, and N. C. Hebert, editors. John Wiley & Sons, New York. 224.
13. BERKINBLIT, M. B., S. A. KOVALEV, V. V. SMOLYANINOV, and L. M. CHAYLAKHYAN. 1971. The electrical behavior of the myocardium as a system and the characteristics of the cellular membrane of the heart. In *Models of the Structural-Functional Organization of Certain Biological Systems*. I. M. Gelfand, V. S. Garfinkel, S. V. Fomin, and M. L. Tsetlin, editors. The M. I. T. Press, Cambridge, Mass. 78.
14. KOOTSEY, J. M. 1975. Voltage clamp simulation. *Fed. Proc.* In press.
15. SOMMER, J. R., and E. A. JOHNSON. 1968. Cardiac muscle: A comparative study of Purkinje fibers and ventricular fibers. *J. Cell Biol.* **36**:497.
16. JOHNSON, E. A., and M. LIEBERMAN. 1971. Heart: Excitation and contraction. *Annu. Rev. Physiol.* **33**:479.
17. LIEBERMAN, M., A. E. ROGGEVEEN, J. E. PURDY, and E. A. JOHNSON. 1972. Synthetic strands of cardiac muscle: Growth and physiological implications. *Science (Wash. D. C.)* **175**:909.
18. PURDY, J. E., M. LIEBERMAN, A. E. ROGGEVEEN, and R. G. KIRK. 1972. Synthetic strands of cardiac muscle: Formation and ultrastructure. *J. Cell Biol.* **55**:563.
19. LIEBERMAN, M., F. J. MANASEK, T. SAWANOBORI, and E. A. JOHNSON. 1973. Cytochalasin B: Its morphological and electrophysiological actions on synthetic strands of cardiac muscle. *Dev. Biol.* **31**:380.
20. LIEBERMAN, M. 1973. Electrophysiological studies of a synthetic strand of cardiac muscle. *Physiologist*. **16**:551.
21. GAGE, P. W., and R. S. EISENBERG. 1969. Capacitance of the surface and transverse tubular membrane of frog sartorius muscle fibers. *J. Gen. Physiol.* **53**:265.
22. KOOTSEY, J. M., and E. A. JOHNSON. 1973. Buffer amplifier with femtofarad input capacity using operational amplifiers. *IEEE (Inst. Electr. Electron. Eng.) Trans Biomed. Eng.* **20**:389.
23. CRANK, J., and P. NICOLSON. 1947. A practical method for numerical evaluations of solutions of partial differential equations of the heat-conduction type. *Proc. Camb. Phil. Soc.* **43**:50.
24. POWELL, M. J. D. 1964. An efficient method of finding the minimum of a function of several variables without calculating derivatives. *Comput. J.* **7**:155.
25. MATSUDA, K. 1960. Some electrophysiological properties of terminal Purkinje fibers of heart. In *Electrical Activity of Single Cells*. Y. Katsuki, editor. Igaku Shoin, Tokyo, Japan. 283.
26. BONKE, F. I. M. 1973. Electrotonic spread in the sinoatrial node of the rabbit heart. *Pflugers Arch. Eur. J. Physiol.* **339**:17.
27. GAGE, P. W., and R. S. EISENBERG. 1969. Action potentials, afterpotentials, and excitation-contraction coupling in frog sartorius fibers without transverse tubules. *J. Gen. Physiol.* **53**:298.
28. TRAUTWEIN, W., and D. G. KASSEBAUM. 1961. On the mechanism of spontaneous impulse generation in the pacemaker of the heart. *J. Gen. Physiol.* **45**:317.
29. VASSALLE, M. 1965. Cardiac pacemaker potentials at different extra- and intracellular K concentrations. *Am. J. Physiol.* **208**:770.
30. ADRIAN, R. H., and L. D. PEACHEY. 1965. The membrane capacity of frog twitch and slow muscle fibres. *J. Physiol. (Lond.)*. **181**:324.
31. PAGE, E. 1962. Cat heart muscle in vitro. III. The extracellular space. *J. Gen. Physiol.* **46**:201.

32. HARSCH, M., and J. W. GREEN. 1963. Electrolyte analyses of chick embryonic fluids and heart tissues. *J. Cell Comp. Physiol.* **62**:319.
33. McDONALD, T. F., and R. L. DEHAAN. 1973. Ion levels and membrane potential in chick heart tissue and cultured cells. *J. Gen. Physiol.* **61**:89.
34. CARMELIET, E., C. R. HORRES, M. LIEBERMAN, and J. S. VEREECKE. 1975. Potassium permeability in the embryonic chick heart: changes with age, external K and valinomycin. In *Developmental and Physiological correlates of Cardiac Muscle*. M. Lieberman and T. Sano, editors. Raven Press, New York N. Y. In press.
35. NIEDERGERKE, R. 1963. Movements of Ca in beating ventricles of the frog heart. *J. Physiol. (Lond.)*. **167**:551.
36. PAGE, S. G., and R. NIEDERGERKE. 1972. Structures of physiological interest in the frog ventricle. *J. Cell Sci.* **11**:179.
37. BURROWS, R., and J. F. LAMB. 1962. Sodium and potassium fluxes in cells cultured from chick embryo heart muscle. *J. Physiol. (Lond.)*. **162**:510.
38. MOBLEY, B. A., and E. PAGE. 1972. The surface area of sheep cardiac Purkinje fibres. *J. Physiol. (Lond.)*. **220**:547.
39. WEIDMANN, S. 1970. Electrical constants of trabecular muscle from mammalian heart. *J. Physiol. (Lond.)* **210**:1041.
40. PAGE, E., and H. A. FOZZARD. 1973. Capacitive, resistive and syncytial properties of heart muscle-ultrastructural and physiological considerations. In *The Structure and Function of Muscle*. G. H. Bourne, editor. Academic Press, Inc., New York. 91.
41. DULHUNTY, A. F., and P. W. GAGE. 1973. Electrical properties of toad sartorius muscle fibres in summer and winter. *J. Physiol. (Lond.)*. **230**:619.
42. HIRAKOW, R. 1970. Ultrastructural characteristics of the mammalian and sauropsidan heart. *Am. J. Cardiol.* **25**:195.
43. JEWETT, P. H., J. R. SOMMER, and E. A. JOHNSON. 1971. Cardiac muscle: Its ultrastructure in the finch and hummingbird with special reference to the sarcoplasmic reticulum. *J. Cell Biol.* **49**:50.
44. SOMMER, J. R., and E. A. JOHNSON. 1969. Cardiac muscle: A comparative ultrastructural study with special reference to frog and chicken hearts. *Z. Zellforsch. Mikrosk. Anat.* **98**: 437.
45. FISCHBACH, G. D., M. NAMEROFF, and P. G. NELSON, 1971. Electrical properties of chick skeletal muscle fibers developing in cell culture. *J. Cell Physiol.* **78**:289.
46. SAKAMOTO, Y., and M. GOTO. 1970. A study of the membrane constants in the dog myocardium. *Jap. J. Physiol.* **20**:30.
47. HYDE, A., B. BLONDEL, A. MATTER, J. P. CHENEVAL, B. FILLOUX, and L. GIRARDIER. 1969. Homo- and heterocellular junctions in cell cultures: An electrophysiological and morphological study. *Prog. Brain Res.* **31**:283.
48. JONGSMA, H. J., and H. E. VAN RIJN. 1972. Electrotonic spread of current in monolayer cultures of neonatal rat heart cells. *J. Membr. Biol.* **9**:341.
49. TOMITA, T. 1966. Membrane capacity and resistance of mammalian smooth muscle. *J. Theor. Biol.* **12**:216.
50. FREYGANG, W. H., and W. TRAUTWEIN. 1970. The structural implications of the linear electrical properties of cardiac Purkinje strands. *J. Gen. Physiol.* **55**:524.
51. SPERELAKIS, N., and D. LEHMKUHL, 1964. Effect of current on transmembrane potentials in cultured chick heart cells. *J. Gen. Physiol.* **47**:895.
52. TASAKI, I., and S. HAGIWARA. 1957. Capacity of muscle fiber membrane. *Am. J. Physiol.* **188**:423.
53. MAUGHAN, D. W. 1973. Some effects of prolonged polarization on membrane currents in bullfrog atrial muscle. *J. Membr. Biol.* **11**:331.
54. CRILL, W. E., R. E. RUMERY, and J. W. WOODBURY. 1959. Effect of membrane current on transmembrane potentials of cultured chick embryo heart cells. *Am. J. Physiol.* **197**:733.
55. LIEBERMAN, M. 1967. Effects of cell density and low K on action potentials of cultured chick heart cells. *Circ. Res.* **21**:879.

56. DEHAAN, R. L., and S. H. GOTTLIEB. 1968. The electrical activity of embryonic chick heart cells isolated in tissue culture singly or in interconnected sheets. *J. Gen. Physiol.* **52**:643.
57. PAPPANO, A. J., and N. SPERELAKIS. 1969. Low  $K^+$  conductance and low resting potentials of isolated single cultured heart cells. *Am. J. Physiol.* **217**:1076.
58. PEPPER, K., and W. TRAUTWEIN. 1968. A membrane current related to the plateau of the action potential of Purkinje fibres. *Pfluegers Archiv. Gesamte Physiol. Menschen Tiere.* **303**:108.
59. EISENBERG, R. S., and E. A. JOHNSON. 1970. Three-dimensional electrical field problems in physiology. *Prog. Biophys. Mol. Biol.* **20**:1.
60. SCHANNE, O., H. KAWATA, B. SCHAFER, and M. LAVALLEE. 1966. A study on the electrical resistance of the frog sartorius muscle. *J. Gen. Physiol.* **49**:897.
61. SCHANNE, O. F., and E. R. P. DE CERETTI. 1971. Measurement of input impedance and cytoplasmic resistivity with a single microelectrode. *Can. J. Physiol. Pharmacol.* **49**:713.
62. LEHMKUHL, D., and N. SPERELAKIS. 1965. Electrotonic spread of current in cultured chick heart cells. *J. Cell. Comp. Physiol.* **66**:119.
63. VALIDOSERA, R., C. CLAUSEN, and R. S. EISENBERG. 1974. Circuit models of the passive electrical properties of frog skeletal muscle fibers. *J. Gen. Physiol.* **63**:432.
64. VEREECKE, J., M. LIEBERMAN, T. SAWANOBORI, E. A. JOHNSON, and W. NEW. 1973. The three-electrode method of voltage clamp in cardiac muscle: A feasibility study. *Physiologist.* **16**:477. (Abstr.).